

# Mini-Project in Mathematical and Computational Modeling

*École Polytechnique Fédérale de Lausanne, Switzerland*

Florian + Dariusz

## Introduction

The periodic changes that come about due to the day-night cycle to things ranging from visibility to temperature create an environment in which it is advantageous to adapt behaviour to this extrinsic period. Perhaps vision becomes so restricted in the night that basic processes like hunting for food or looking for mates become so inefficient that it's a better strategy to conserve energy when it's dark. Perhaps the opposite is the case and hunting during the night becomes an advantage due to specially evolved senses in animals such as bats.

For this reason many different lifeforms, from bacteria to animals, have adapted to the 24 hour period that exists around them by synchronising behaviour and processes in different tissues to the day-night cycle by keeping track of time using internal 'clocks'.

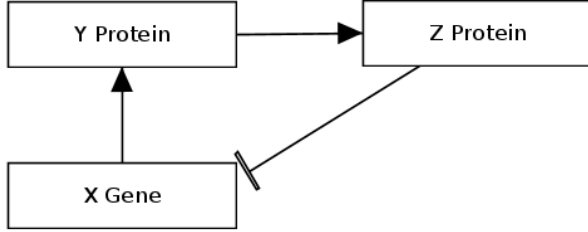
In humans this clock works by having a part of the brain, called the suprachiasmatic nuclei (SCN), manage the production of several clock proteins in such a way as to create oscillatory patterns in the concentration of these proteins. Negative feedback loops are used in such a way as to create a periodic rise and fall in the production of proteins that can be influenced by external factors such a light intensity and food uptake to regularly adjust the synchronisation to new environments.

## The Model

In this simplified model of the SCN we do not take into account such outside signals and instead focus on behaviours of cells in the SCN all by themselves. The model looks at the production of clock gene mRNA (designated as X), which leads to production of a clock protein(Y). This clock gene protein activates transcription of a third compound (Z), which acts as a transcriptional inhibitor of X, thus creating a negative feedback loop.

In this report we examine several conditions that need to be met for this simple model to exhibit circadian oscillations in the concentrations of the compounds involved. This model is then expanded to investigate synchronisation between cells by taking into account a third protein (V) that is exported and allows the cells in the SCN to talk to each other. First taking into account only 2 cells, this model is expanded to hundreds of cells later on, not reaching the human population of cells in the SCN of 10'000, but at least providing a smaller model that could be scaled up to that number if more processing power was available.

# Part A - One-Cell Model

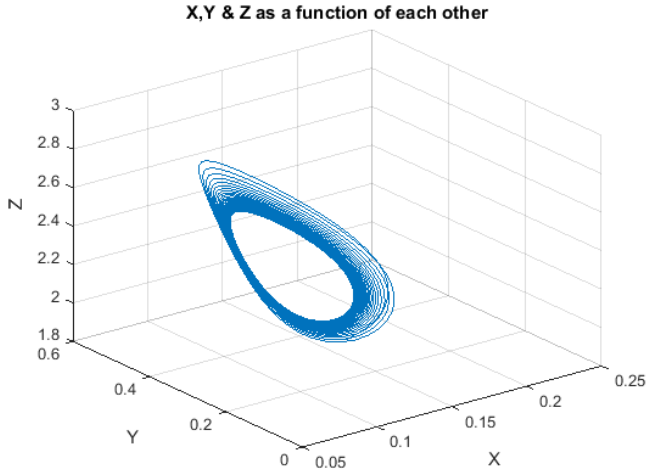


(a) One-Cell Model

The gene mRNA  $X$  codes for protein  $Y$  which, in turn, activates transcriptional inhibitor  $Z$ . The resulting model behaves as a three-variable oscillator.

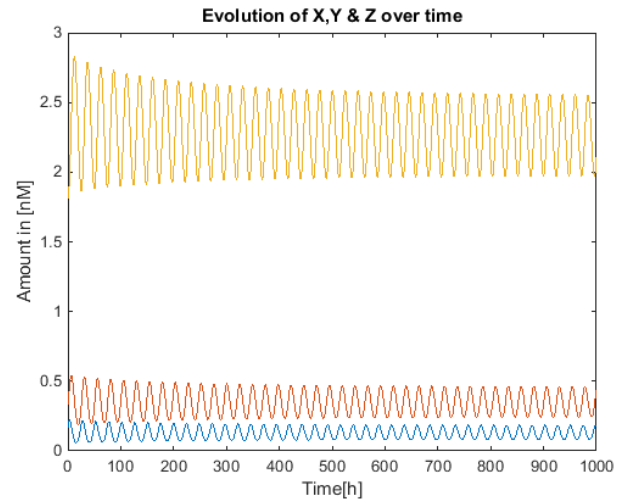
$$\begin{aligned}\frac{\delta X}{\delta t} &= v_1 \frac{K_1^n}{K_1^n + Z^n} - v_2 \frac{X}{K_2 + X} \\ \frac{\delta Y}{\delta t} &= k_3 X - v_4 \frac{Y}{K_4 + Y} \\ \frac{\delta Z}{\delta t} &= k_5 Y - v_6 \frac{Z}{K_6 + Z}\end{aligned}$$

|       |                           |       |                           |
|-------|---------------------------|-------|---------------------------|
| $v_1$ | translation rate of $X$   | $K_1$ | Michaelis constant of $X$ |
| $v_2$ | degradation rate of $X$   | $K_4$ | Michaelis constant of $Y$ |
| $v_4$ | degradation rate of $Y$   | $K_6$ | Michaelis constant of $Z$ |
| $v_6$ | degradation rate of $Z$   |       |                           |
| $k_3$ | transcription rate of $X$ |       |                           |
| $k_5$ | transcription rate of $Z$ |       |                           |



(a) Trajectories

The limit cycle is reached as the variations of  $X(t)$ ,  $Y(t)$  and  $Z(t)$  become fixed : The trajectories converge, non-linearly (the distance between similar trajectories aren't regular) towards an ellipse (where the blue stripes accumulate)



(b) Frequency spectrum

The amplitude of the three variations stabilize after a few hundred hours. The signal are not in phase but have the same, regular, frequencies.

Figure 3:

Trajectories of  $X(t)$ ,  $Y(t)$  and  $Z(t)$  with initial conditions :  $X_0 = 0.16$ ,  $Y_0 = 0.33$ ,  $Z_0 = 1.8$  [nM]

We observe on both graphs that  $Z(t)$  has the bigger amplitude of variation whereas  $X(t)$  and  $Y(t)$  have small amplitudes. Additionally, the convergence towards a single loop in (a) indicate that the frequencies of the signals are equal; this is illustrated as well in (b)

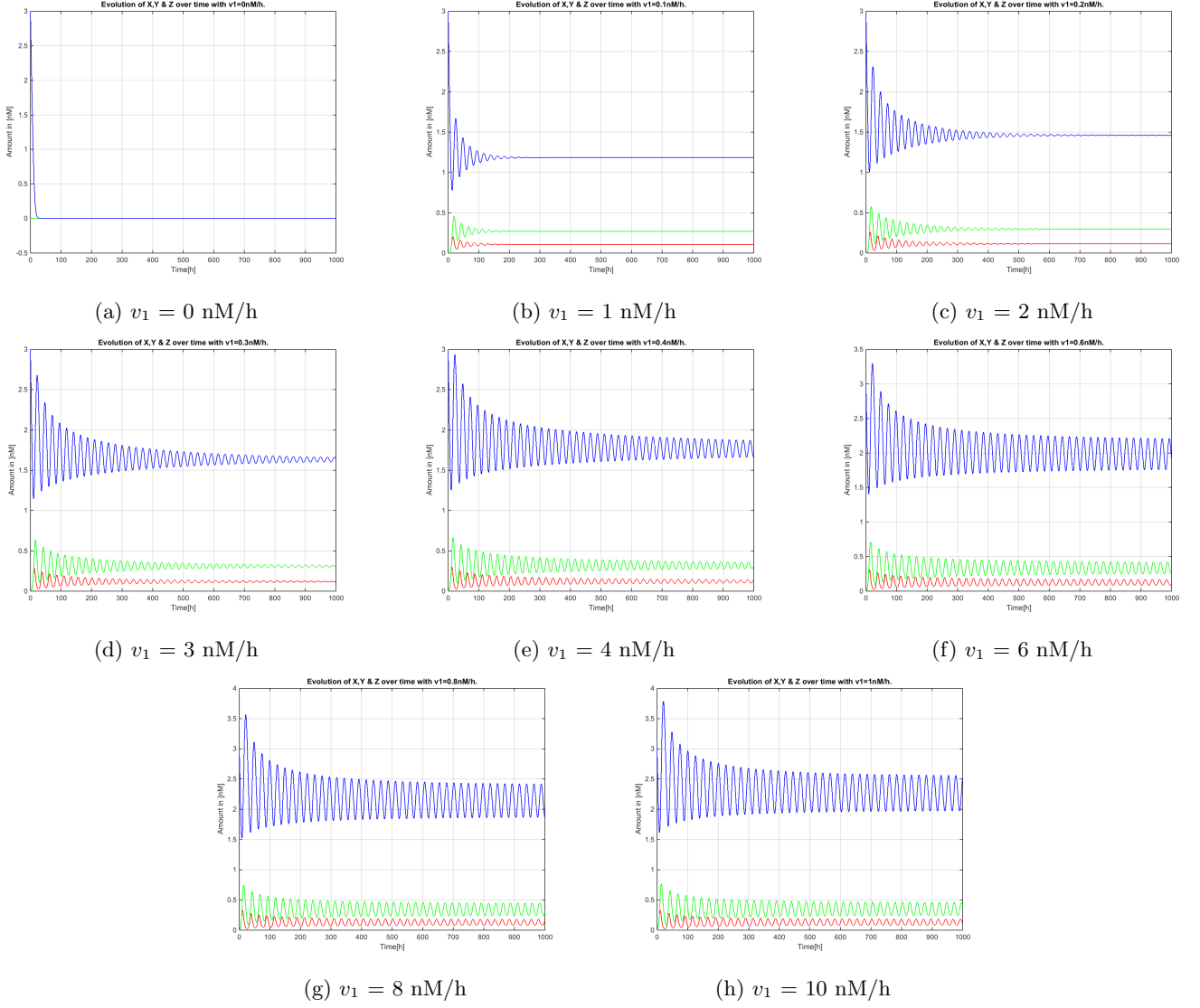


Figure 4:  $X(t)$ ,  $Y(t)$  and  $Z(t)$  with initial conditions  $X_0 = 0.16$ ,  $Y_0 = 0.33$ ,  $Z_0 = 1.8$  [nM]  
The first signal to fade is  $Y(t)$  and its oscillatory stability predicts stability of the system. We also observe that the signals converge towards null or the limit cycle in a non-linear fashion. **At the opposite, it is rather difficult to predict the threshold value of  $v_1$  using those plots ?**

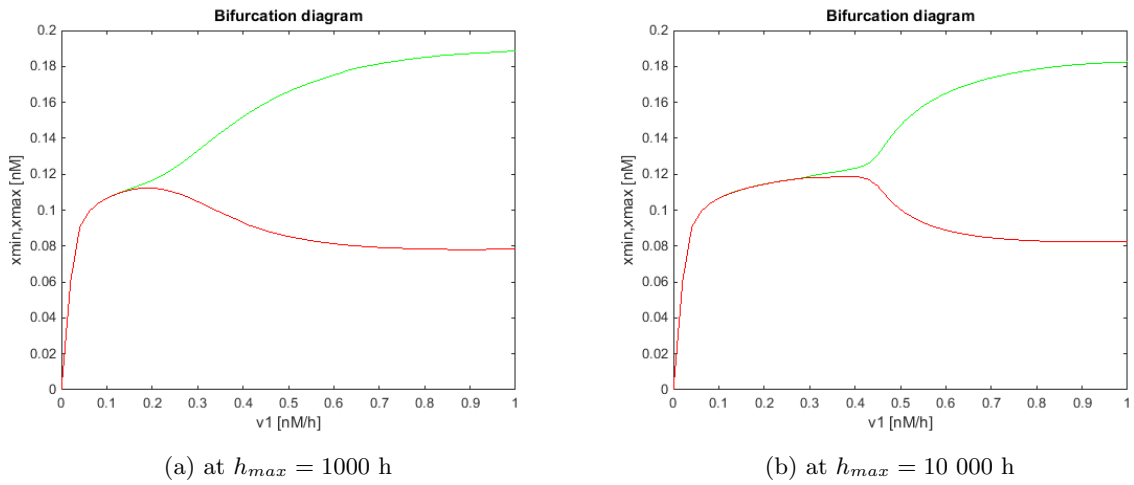


Figure 5: Bifurcation Diagram :  $X_{min}$  and  $X_{max}$  plotted at time intervals  $[9/10; 1]$  of  $h_{max}$   
A limit cycle might be reached when  $X_{min} \neq X_{max}$ . However, the system needs to be run for enough time for the cycle to be reached, as the (a) suggests. (b) illustrates the non-linear convergence of the system; also the threshold for  $v_1$  seems to be around 4.5

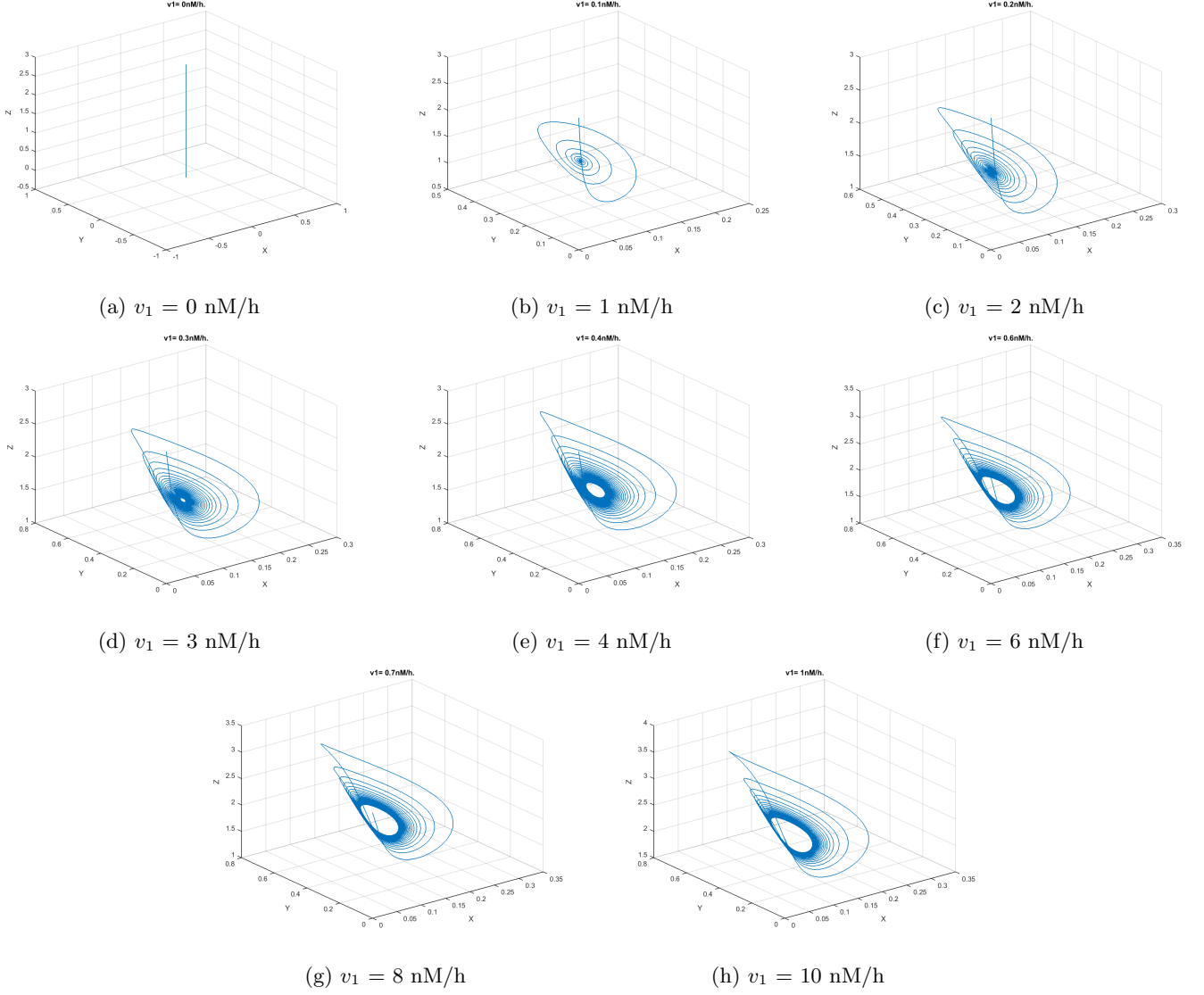


Figure 6: Trajectories when varying  $v_1$  with initial conditions  $X_0 = 0.16$ ,  $Y_0 = 0.33$ ,  $Z_0 = 1.8$  [nM].  $v_1$  has to reach a certain value for  $X(t)$  to be able to compensate its inhibition by  $Z(t)$  and therefore for the system to reach a limit cycle. We observe that this value is slightly greater than 4nM/h, as the trajectories still converge to null in (e); there is an 'eye', even though it is smaller than in (f) and (g), since the timescale is not big enough to let the system dissipate completely.

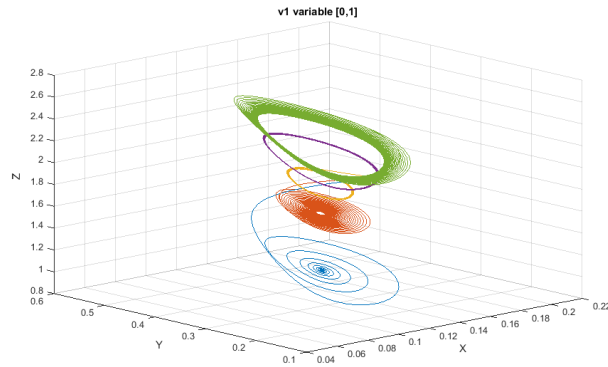
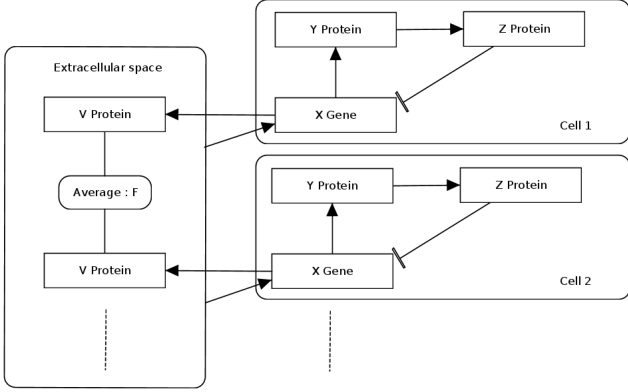


Figure 7: Superimposed trajectories at late timepoints with initial conditions  $X_0 = 0.16$ ,  $Y_0 = 0.33$ ,  $Z_0 = 1.8$  [nM] and  $v_1 = 0.1/0.3/0.5/0.7/0.9$  nM/h. We observe here that  $Z(t)$  tends to reach greater concentration stability with increasing  $v_1$ .

# Part B - Multiple Cells Model



(a) Multiple Cells Model

The gene  $X$  codes for protein  $Y$  which, in turn, activates transcriptional inhibitor  $Z$ . In addition, gene  $X$  activates a positive feedback loop through the mean concentration of extracellular protein  $V$

$$\frac{\delta X}{\delta t} = v_1 \frac{K_1^n}{K_1^n + Z^n} - v_2 \frac{X}{K_2 + X} + v_c \frac{KF}{K_c + KF}$$

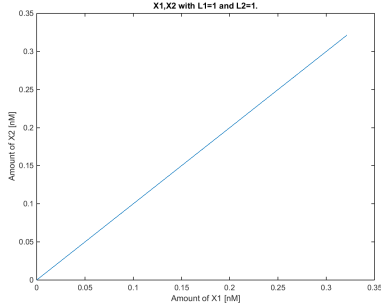
$$\frac{\delta Y}{\delta t} = k_3 X - v_4 \frac{Y}{K_4 + Y}$$

$$\frac{\delta Z}{\delta t} = k_5 Y - v_6 \frac{Z}{K_6 + Z}$$

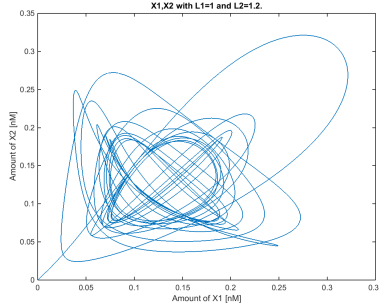
$$\frac{\delta V_i}{\delta t} = k_7 X_i - v_8 \frac{V_i}{K_8 + V_i}$$

$$\text{where } F = \frac{1}{N} \sum_{i=1}^N V_i$$

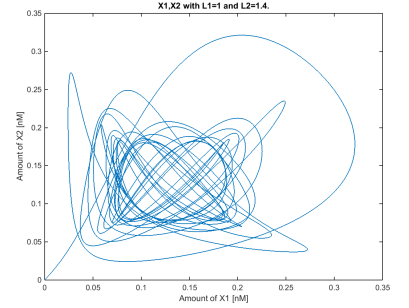
|       |                           |       |                           |
|-------|---------------------------|-------|---------------------------|
| $v_1$ | translation rate of $X$   | $k_7$ | transcription rate of $V$ |
| $v_2$ | degradation rate of $X$   | $k_1$ | transcription rate of $X$ |
| $v_4$ | degradation rate of $Y$   | $K_4$ | Michaelis constant of $Y$ |
| $v_6$ | degradation rate of $Z$   | $K_6$ | Michaelis constant of $Z$ |
| $v_8$ | degradation rate of $V$   | $K_8$ | Michaelis constant of $V$ |
| $k_3$ | transcription rate of $X$ | $K$   | Coupling Constant         |
| $k_5$ | transcription rate of $Z$ |       |                           |



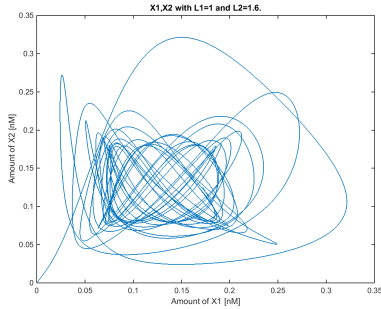
(a)  $\lambda_1 = 1, \lambda_2 = 1 [h^{-1}]$



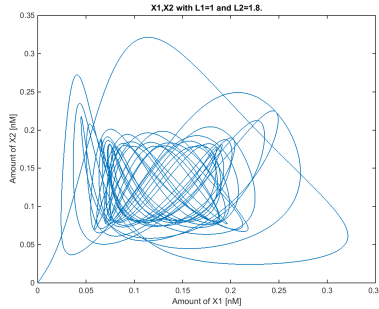
(b)  $\lambda_1 = 1, \lambda_2 = 1.2 [h^{-1}]$



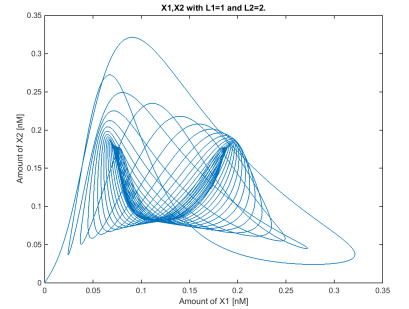
(c)  $\lambda_1 = 1, \lambda_2 = 1.4 [h^{-1}]$



(d)  $\lambda_1 = 1, \lambda_2 = 1.6 [h^{-1}]$



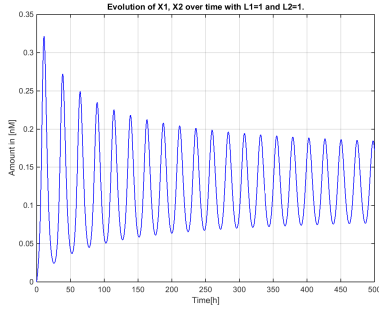
(e)  $\lambda_1 = 1, \lambda_2 = 1.8 [h^{-1}]$



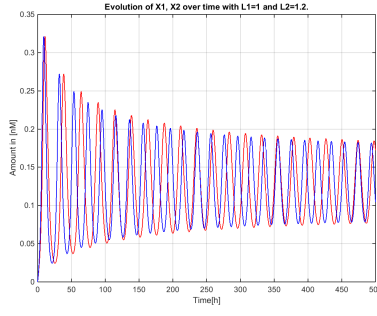
(f)  $\lambda_1 = 1, \lambda_2 = 2 [h^{-1}]$

Figure 10:  $X_1$  and  $X_2$  trajectories with varying  $\lambda_i$  in a two-cells Model

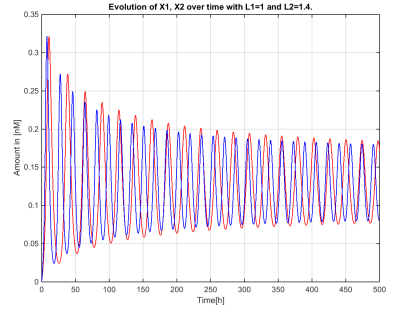
I don't really know what to say except 'wow it's cool' + square is max/min of  $X_s$



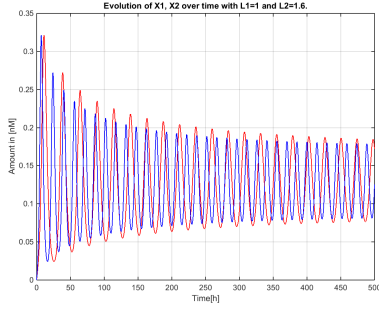
(a)  $\lambda_1 = 1, \lambda_2 = 1 [h^{-1}]$



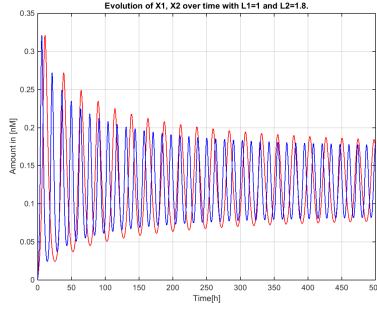
(b)  $\lambda_1 = 1, \lambda_2 = 1.2 [h^{-1}]$



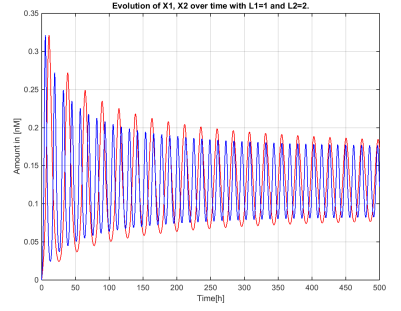
(c)  $\lambda_1 = 1, \lambda_2 = 1.4 [h^{-1}]$



(d)  $\lambda_1 = 1, \lambda_2 = 1.6 [h^{-1}]$

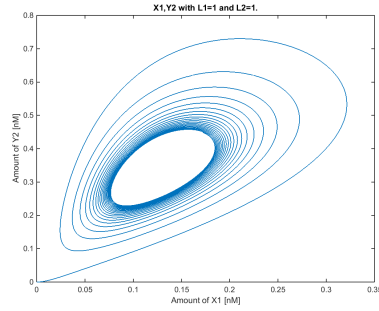


(e)  $\lambda_1 = 1, \lambda_2 = 1.8 [h^{-1}]$

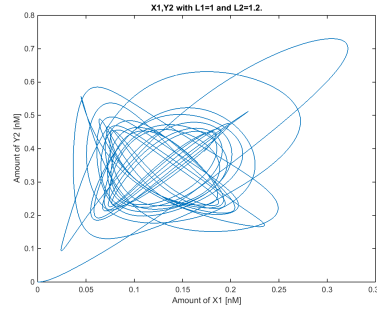


(f)  $\lambda_1 = 1, \lambda_2 = 2 [h^{-1}]$

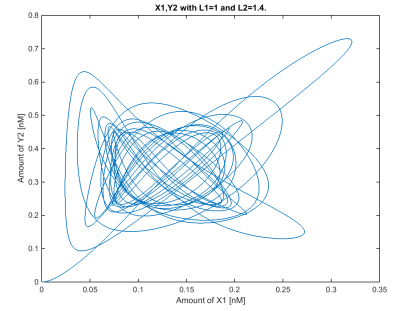
Figure 11:  $X_1(t)$  and  $X_2(t)$  trajectories in a two-cells Model  
We observe that



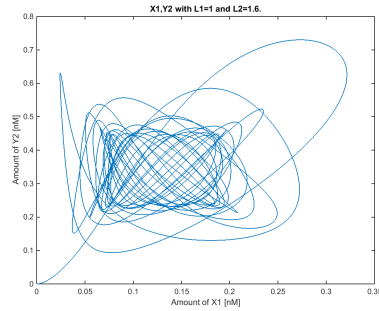
(a)  $\lambda_1 = 1, \lambda_2 = 1 [h^{-1}]$



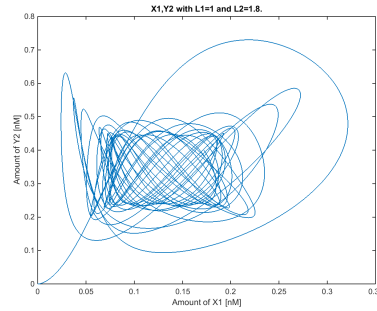
(b)  $\lambda_1 = 1, \lambda_2 = 1.2 [h^{-1}]$



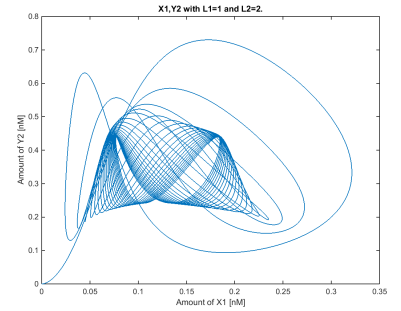
(c)  $\lambda_1 = 1, \lambda_2 = 1.4 [h^{-1}]$



(d)  $\lambda_1 = 1, \lambda_2 = 1.6 [h^{-1}]$

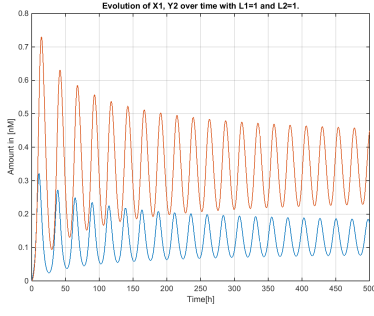


(e)  $\lambda_1 = 1, \lambda_2 = 1.8 [h^{-1}]$

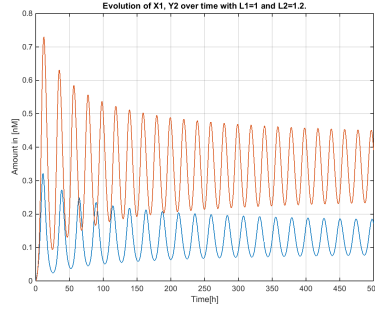


(f)  $\lambda_1 = 1, \lambda_2 = 2 [h^{-1}]$

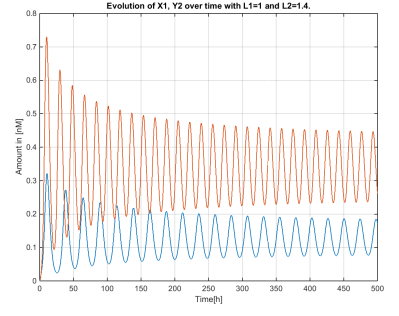
Figure 12:  $X_1$  and  $Y_2$  trajectories



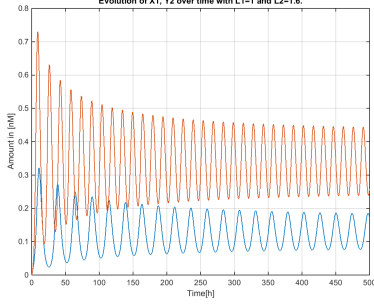
(a)  $\lambda_1 = 1, \lambda_2 = 1 [h^{-1}]$



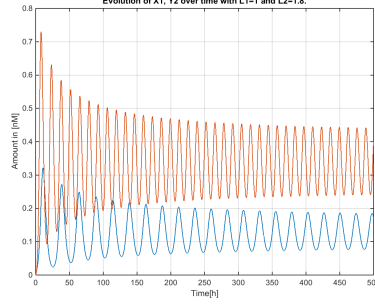
(b)  $\lambda_1 = 1, \lambda_2 = 1.2 [h^{-1}]$



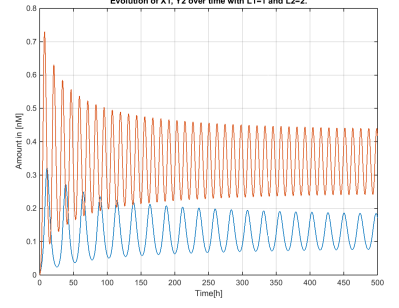
(c)  $\lambda_1 = 1, \lambda_2 = 1.4 [h^{-1}]$



(d)  $\lambda_1 = 1, \lambda_2 = 1.6 [h^{-1}]$

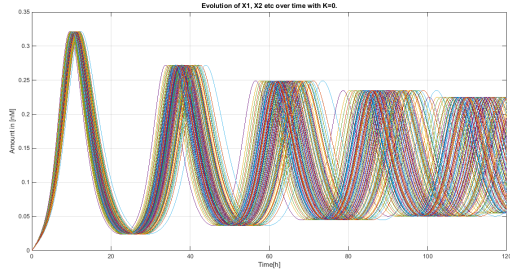


(e)  $\lambda_1 = 1, \lambda_2 = 1.8 [h^{-1}]$

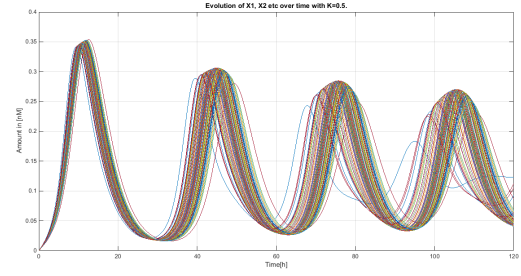


(f)  $\lambda_1 = 1, \lambda_2 = 2 [h^{-1}]$

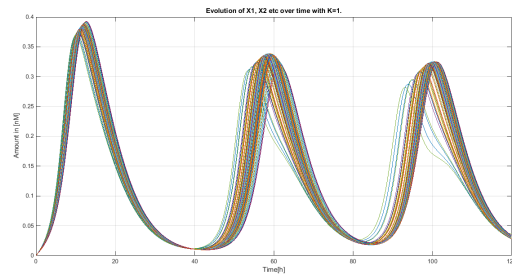
Figure 13: raraara



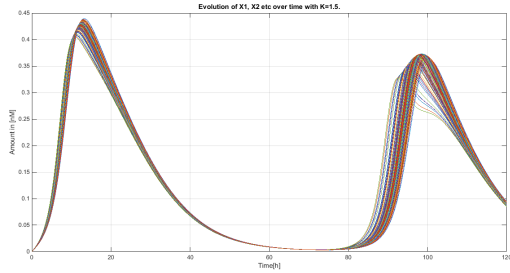
(a)  $K = 0.0$



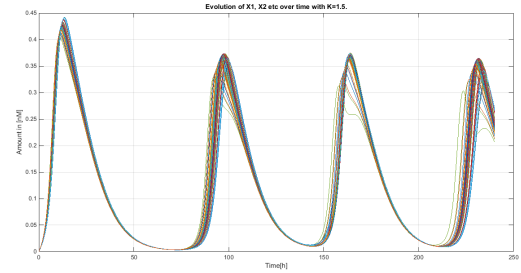
(b)  $K = 0.5$



(c)  $K = 1.0$

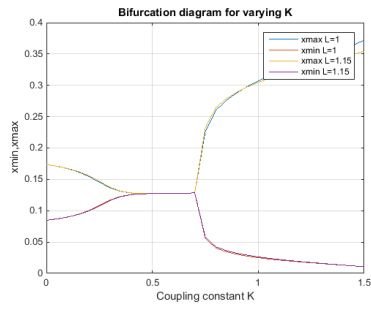


(d)  $K = 1.5$

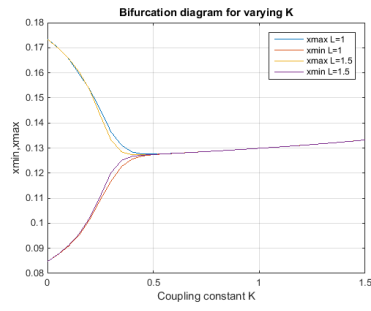


(e)  $K = 1.5$

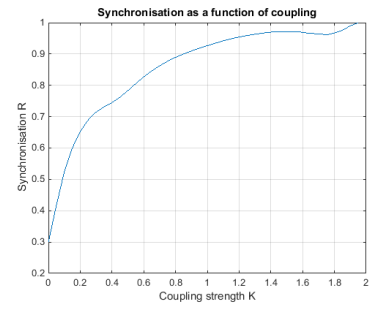
Figure 14: raraara



(a)  $K = 0.0$



(b)  $K = 0.3$



(c)  $K = 1.0$

Figure 15: raraara